NANO LETTERS

2008
Vol. 8, No. 2
431−436

The Role of NiO_x Overlayers on Spontaneous Growth of $NiSi_x$ Nanowires from Ni Seed Layers

Kibum Kang, Sung-Kyu Kim, Cheol-Joo Kim, and Moon-Ho Jo*

Department of Materials Science and Engineering, Pohang University of Science and Technology (POSTECH), San 31, Hyoja-Dong, Nam-Gu, Pohang, Gyungbuk 790-784, Korea

Received September 11, 2007; Revised Manuscript Received November 7, 2007

ABSTRACT

We report a controllably reproducible and spontaneous growth of single-crystalline $NiSi_x$ nanowires using NiO_x/Ni seed layers during SiH_4 chemical vapor deposition (CVD). We provide evidence that upon the reactions of SiH_4 (vapor)–Ni seed layers (solid), the presence of the NiO_x overlayer on Ni seed layers plays the key role to promote the spontaneous one-dimensional growth of $NiSi_x$ single crystals without employing catalytic nanocrystals. Specifically, the spontaneous nanowire formation on the NiO_x overlayer is understood within the frame of the SiH_4 vapor-phase reaction with out-diffused Ni from the Ni underlayers, where the Ni diffusion is controlled by the NiO_x overlayers for the limited nucleation. We show that single-crystalline $NiSi_x$ nanowires by this self-organized fashion in our synthesis display a narrow diameter distribution, and their average length is set by the thickness of the Ni seed layers. We argue that our simple CVD method employing the bilayers of transition metal and their oxides as the seed layers can provide implication as the general synthetic route for the spontaneous growth of metal–silicide nanowires in large scales.

In the catalyst-assisted syntheses of one-dimensional nanocrystals, the metal catalytic nanoparticles are the prerequisites for the dimensionally confined nucleation and the subsequent one-dimensional crystal growth.[1,2] By serving as alloy liquids[1,2] or solid solutions,[3] these metal catalytic nanoparticles mediate the catalytic crystallization by providing lower activation energy for given reactions at lower temperatures than the melting points of given crystals. By contrast, the synthetic routes for nanowires without the presence of the metal nanoparticles can be also available,[4,5] and one class of such examples recently investigated is the vapor-phase syntheses of various silicide nanowires. Although the first synthesis of silicide nanowires were prepared by solid-state reactions between individual Si nanowires and thin Ni overshells,[6] several vapor-phase synthetic routes to spontaneously form various single-crystalline silicide nanowires have been recently reported.[7−14] These spontaneous growth methods for various silicide nanowires can be classified into two schemes: the first scheme employs silicon vapor deposition on transition-metal thin films,[7−9] and the second involves various metal−vapor-phase reactions with silicon substrates.[10−14] Therein they commonly observed the one-dimensional crystallization of silicides without the presence of the catalytic metal nanoparticles self-seeded from the metal or Si thin films. We have also demonstrated that one can direct the dimensionality of $NiSi_x$ from thin films to nanowires on predeposited Ni thin films during SiH_4 chemical vapor deposition (CVD) in the low supersaturation limit of SiH_4 vapors.[9] Such one-dimensional crystal growth via self-catalytic vapor−solid reactions using a simple SiH_4 CVD on the metal surfaces is an interesting scheme, particularly because it can offer practical advantages to produce single-crystalline nanowires in large scales using conventional Si processing techniques to be easily integrated into Si-based electronics. Nevertheless, the growth mechanism of this spontaneous nanowire formation is not well understood, and it is mainly because controllably reproducible synthetic methods are not available to date. Here, we provide experimental evidence that the presence of the oxide overlayer on Ni seed layers significantly promotes the spontaneous one-dimensional growth of $NiSi_x$ single-crystals in a robustly reproducible manner. Specifically, the spontaneous nanowire growth on the NiO_x overlayer in this study is understood with the SiH_4 vapor-phase reaction with Ni out-diffused from the Ni underlayer, where the Ni supply is controlled by NiO_x for the limited nucleation during the SiH_4−Ni reactions. We also show that single-crystalline $NiSi_x$ nanowires by this self-organized manner display a narrow diameter distribution and a defined length distribution set by predeposited Ni thickness.

We start off our syntheses with thermally evaporated Ni thin films of 80 nm in thickness on SiO_2/Si substrates. The

* Corresponding author. E-mail: mhjo@postech.ac.kr.

10.1021/nl072326c CCC: $40.75
Published on Web 01/12/2008

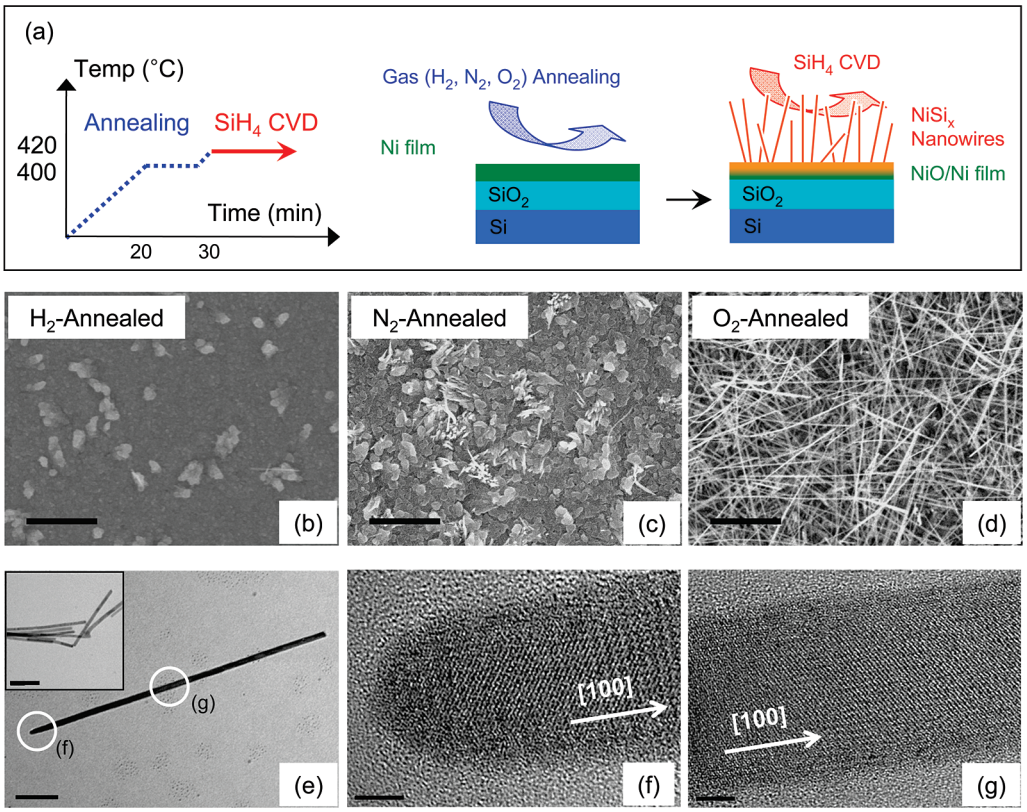

Figure 1. (a) The schematics of the spontaneous nanowire growth in this study. **(**b−d) The representative SEM images of the reaction products on H_2-, N_2-, and O_2-annealed samples, respectively. The scale bar is 1 μm. **(**e**)** TEM image of an individual $NiSi_x$ nanowire. Nanowires in the inset exhibit a relatively uniform distribution of diameters. The scale bar is 100 nm. **(**f,g**)** High-resolution TEM images of panel e at the different locations marked with circles, showing the crystal orientation along the length is [100]. The acute-angled tip at the end of the nanowires shows the absence of any catalyst tip. The scale bar is 3 nm.

Ni thin films are subsequently loaded into a quartz-tube furnace, where we carry out CVD of SiH_4 (specifically, 10% of SiH_4 diluted in high purity H_2) below the thermal decomposition temperature of SiH_4. Figure 1a shows the schematics of our syntheses; the furnace temperature was raised to the growth temperature of 400 °C, and the thermally evaporated Ni films were annealed in the presence of various gases such as H_2, N_2, or O_2 for 10 min before each SiH_4 CVD process. Figure 1b−d is the representative plan-view of scanning electron microscope (SEM) images of the reaction products using 50 Torr of SiH_4 at 420 °C for 15 min on annealed samples in H_2, N_2, or O_2 for 10 min, respectively. Our synthetic approach exploits Ni-catalyzed decomposition of SiH_4, which can occur well below the thermal decomposition temperature of SiH_4 at above 600 °C,[15] and from all the samples we commonly identified the formation of $NiSi_x$ phases on the surfaces. Interestingly, however, we found the significantly distinctive surface morphologies of $NiSi_x$ from different gas-annealing procedures before the SiH_4 CVD. In particular, we observed a high density of $NiSi_x$ nanowires from the O_2-annealed sample with the remarkable contrasts from the H_2-annealed sample with $NiSi_x$ planar sheets along with large $NiSi_x$ grains. The N_2-annealed sample displays mixed features with large grains of $NiSi_x$ and few embryonic nanowires. We emphasize here that these growth characteristics per different gas-annealing processes are robustly reproducible, and with the presence of Ni oxide overlayers we observed this spontaneous nanowire growth regardless of the choice of substrates we employed, such as glass and indium tin oxides. The transmission electron microscope (TEM) images in Figure 1e−g demonstrate that the nanowires are single-crystalline $NiSi_x$, and this particular nanowire shows the [100] crystallographic orientation of Ni_2Si along the wire axis, despite that the crystallographic phases and the growth orientation differ from nanowire to nanowire. We analyzed four representative nanowires with electron diffraction patterns and found three out of four were Ni_2Si phases and the other was a NiSi phase; also, see Supporting Information (S1 and S2) for more thorough TEM diffraction analyses along with their high-resolution images. From many nanowires as typically shown in Figure 1f, we found that the acute-angled tips without the presence of any catalyst tip at the end of the nanowires that is the typical characteristic of the catalytic nanowire syntheses.[1] The average diameters of the synthesized nanowires are typically ranged from 10 to 15 nm in diameter with a relatively narrow distribution, as shown in the inset of Figure 1e.

The most prominent feature in Figure 1b−d (that whether the reaction products of $NiSi_x$ are sheets or nanowires) can be inferred from the modification of the chemical state of Ni surfaces during the H_2- and O_2-annealing steps. The chemical states of the Ni surfaces at atmospheric conditions have been extensively investigated for its wide use as

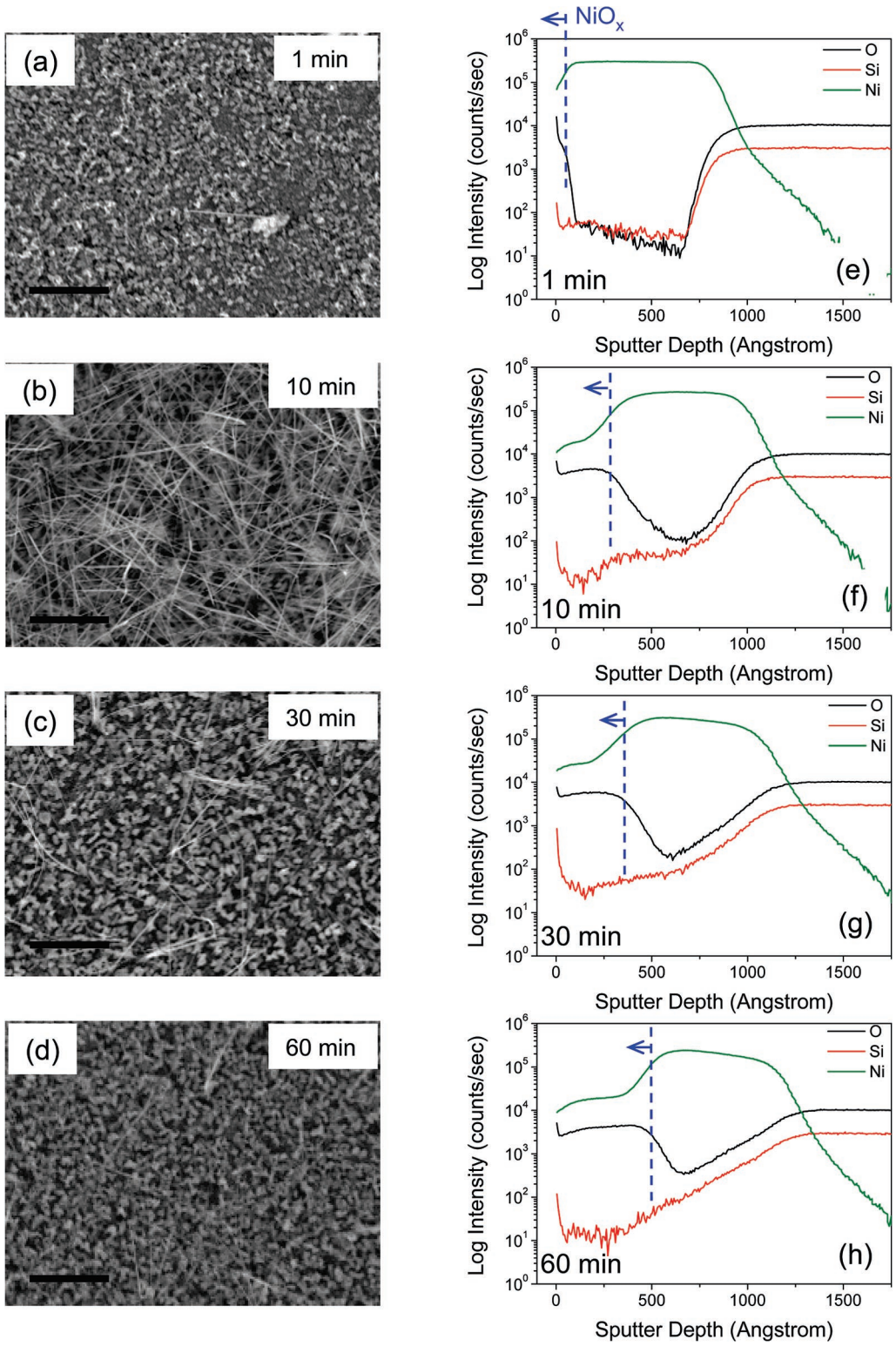

Figure 2. Series of plan-view SEM images of samples where the NiO_x thickness varies by oxidizing the 80 nm thick Ni thin films for (a) 1, (b) 10, (c) 30 and (d) 60 min at 100 Torr of O_2, respectively. The scale bar is 1 μm. (e−h) The corresponding series of secondary ion mass spectrometer depth profiles before the nanowire growth, respectively.

catalysts,[16] and in our synthesis procedure we identified it covered with the native oxide of Ni by secondary ion mass spectrometer (SIMS). The O_2 annealing for 10 min further oxidizes Ni surfaces by a significant amount and leaves its oxide of 20−30 nm in thickness, as verified by SIMS in Figure 2f; note that the estimated thickness from SIMS data is only provisional due to rough surfaces and interfaces and thus roughly represents the upper limit. To the contrary, during the H_2 annealing the native oxide is reduced by H_2, which is also very well known,[16] and the bare Ni surfaces are exposed to SiH_4 vapors during the subsequent CVD growth; see also Supporting Information (S5). We also note

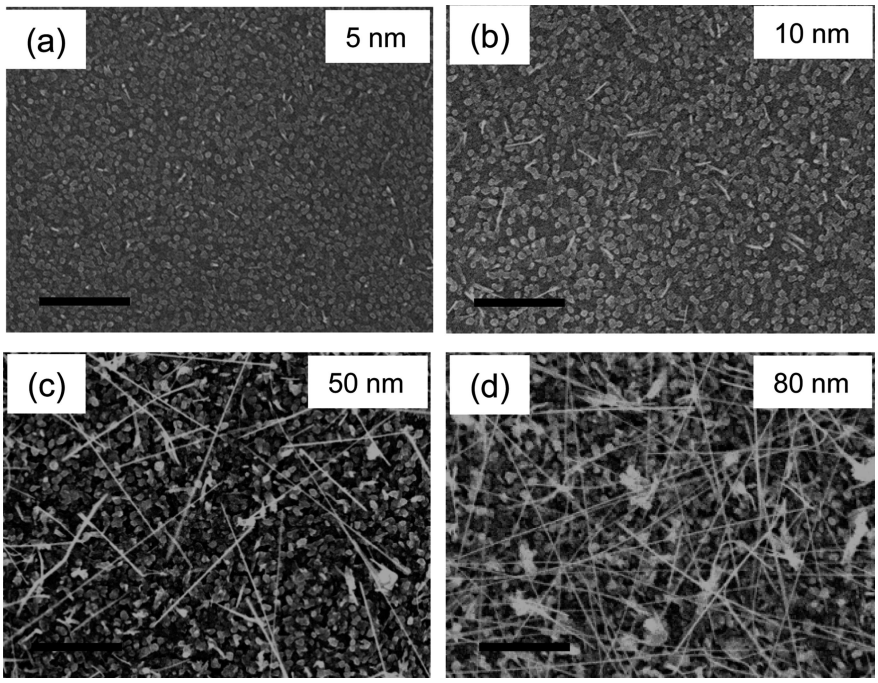

Figure 3. Series of plan-view SEM images of samples where the Ni underlayer thickness of **(**a**)** 5, **(**b**)** 10, **(**c**)** 50, and **(**d**)** 80 nm are oxidized for the constant period of time of 10 min. The scale bar is 1 μm.

that there is a persistent reducing agent of H_2 during the CVD growth as well, because our SiH_4 process gas is 10% diluted in H_2. Thus, it is clear that the spontaneous nanowire growth in our observations is directly related to the presence of Ni oxide overlayers on Ni surfaces. To this end we further investigated these unique growth characteristics around the critical role of the NiO_x/Ni seed layers. Specifically, we then carried out the $NiSi_x$ nanowire growth varying the thickness of NiO_x overlayers and Ni seed layers independently with the close observations of the nanowire density and the average length. Figure 2a−d shows a series of SEM images of samples where the NiO_x thickness varies by oxidizing the 80 nm thick Ni thin films for 1, 10, 30, and 60 min at 100 Torr of O_2, respectively. As verified in Figure 2e−h, the corresponding series of SIMS depth profiles before the nanowire growth indeed show that the thickness of NiO_x increases by increasing oxidation time. We also note that there is significant intermixing of Ni and SiO_2 increasing NiO_x upon longer oxidations. Interestingly, we found that the maximum density of nanowires is achieved by 10 min oxidation, and the O_2 annealing below and above 10 min significantly reduces the nanowire density. In fact, only the short nanowires with a scarcely scattered density are observed from both the samples of thinner or thicker NiO_x films by shorter or longer oxidation than 10 min. In turn, Figure 3a−d shows the growth characteristics when varying the thickness of Ni seed layers oxidized for the constant period of time of 10 min, followed by 30 min SiH_4 CVD. The density and length of $NiSi_x$ nanowires are strongly dependent on the Ni thickness as well; they linearly increase upon increasing Ni thickness from 5 nm up to 80 nm. However, we have not observed much difference in the density and length of $NiSi_x$ nanowires when the Ni thickness is above 80 and up to 300 nm; see also Supporting Information (S4). Considering the 10 min oxidation forms the NiO_x overlayers of 20−30 nm in thickness, as shown in Figure 2b,f, we speculate that Ni thin films in the samples of Figure 3a,b are almost fully oxidized with little content of pure Ni upon the SiH_4 CVD. We have only observed that the short nanowires with a small density are present in the samples of thinner Ni films than 10 nm, and that the density and the length of these nanowires remain almost constant even for the longer growth time.

On the basis of our experimental observations, we now further discuss the growth behavior of $NiSi_x$ nanowires in the context of vapor (SiH_4) solid (Ni) reactions, around the role of NiO_x overlayers in particular. The importance of oxides was pointed out in earlier reports of several silicide nanowires[13,17,18] and Si nanowires[19] by vapor transport syntheses where highly reactive oxide species might act as catalysts. In our study, however, the oxides are rather too thick for any catalytic function and we do not see any direct relevance to our case. Our observations that the $NiSi_x$ nanowire density is maximized at a certain thickness of NiO_x can be summarized into at least two rationales; first the $NiSi_x$ nanowires in our synthesis tend not to grow on stand-alone NiO_x seed layers, and second the appropriate condition for the spontaneous nanowire growth requires a combination of NiO_x/Ni seed layers, where the NiO_x thickness should be optimized on the top of Ni underlayers. The chemical reactions to produce $NiSi_x$ nanowires in our synthesis may involve multiple reactions due to the presence of both NiO_x and Ni in series, and the complications of their silicidations. For simplicity, two plausible reaction paths can be surmised here as

$$SiH_4\,(g) + Ni\,(s) \rightarrow NiSi\,(s) + 2H_2\,(g) \qquad (1)$$

and/or

$$SiH_4\,(g) + 2Ni\,(s) \rightarrow Ni_2Si\,(s) + 2H_2\,(g) \qquad (2)$$

SiH_4 (g) is 10% diluted in H_2, therein. Whether Ni is originally supplied from the surface NiO_x layers by H_2 reduction or the Ni seed layers underneath cannot be directly determined. Nevertheless the observation that $NiSi_x$ nanowires do not spontaneously grow on thicker NiO_x overlayers on Ni or stand-alone NiO_x layers suggests that they are produced by the reaction of gas-phase SiH_4 with Ni supplied from the Ni layers. This is also consistent with our observations that the length of $NiSi_x$ nanowires remains constant for the extended growth time up to 30 min in the samples of the very thin Ni (below 15 nm), which can be inferred to the fact that the Ni supply from the Ni seed layers is depleted due to the finite amount. Otherwise, we would expect that nanowires grow longer with a higher density by consuming Ni reduced from NiO_x during the reaction. Indeed, we verified that the length of $NiSi_x$ nanowires can be determined with the preset amount of Ni seed layers, as shown in Figure 4. With the 5 min growth from the NiO_x/Ni seed layers, where the Ni thickness varies from 5 to 80 nm, the average nanowire length proportionally increases, as in Figure 4a. We comment here that for the longer growth than 5 min on the thicker Ni samples above 15 nm the nanowire length is typically above few microns at a very higher density, and it is technically impossible to statistically measure their length distribution with SEM images. Instead, when the Ni thickness is below 15 min the average nanowire length is measurable, and we observed that the nanowire length starts to saturate for the longer growth, as shown in Figure 4b. We also found that with increasing Ni thickness from 5 to 10 and 15 nm, the length of nanowires saturates at the longer length. In the solid−solid reactions of Ni and Si at the intermixing interfaces, it is generally accepted that the reaction occurs by thermally activated diffusion of Ni and Si, and Ni is the faster diffuser.[20,21] Ni diffusion through NiO_x is well understood and it occurs via the O vacancies in the NiO_x lattices, and it can also migrate via grain boundaries or dislocations in NiO_x at elevated temperatures.[22] The cross-sectional TEM images of NiO_x/Ni layers prepared by 10 min oxidation in Figure 5 shows that NiO_x layers are polycrystalline with irregular grains of few nanometers in size. In our synthesis, it is therefore reasonable to conclude that the surface reaction of out-diffused Ni from Ni seed layers with SiH_4 vapor is responsible for the spontaneous growth of $NiSi_x$ nanowires. We speculate that the limited diffusion pathways of Ni in NiO_x are further developed during the SiH_4 CVD growth as a result of NiO_x reductions by H_2 that is supplied both from the reactions of (1) and (2), and/or the background H_2 of SiH_4 precursors; see also Supporting Information (S3 and S6).

In vapor-phase syntheses of various nanowires, the relative low supersaturation degree in the vapor-phase favors one-dimensional morphologies due to the limited nucleation, whereas the relatively higher supersaturation leads to the bulk morphology due to the homogeneous nucleation.[4] This growth behavior is indeed observed in our previous report on the SiH_4 (g)−Ni (s) reactions, where we have observed the spontaneous NiSi nanowire growth in the low supersaturation degree in the vapor-phase of SiH_4 on bare Ni thin films.[9] Whereas the present study provided that Ni for the SiH_4 (g)−Ni (s) reactions is supplied from the Ni layers underneath the NiO_x overlayers, the role of polygrained NiO_x overlayers in our synthesis can be regarded as a diffusion barrier to kinetically and spatially control the out-diffusing Ni supply from Ni films underneath at a given thickness. Then the spontaneous nanowire formation can be understood with the unique role of NiO_x on the limited nucleation by controlling the limited diffusion supply of Ni at an optimally low supersaturation of solid-phase Ni for the vapor-solid reactions. On the other hand, the thin film morphology of $NiSi_x$ is preferred at the relatively high supersaturation of Ni by unlimited Ni supply across the minimum thickness of NiO_x, as shown in Figure 2a, or from the highly H_2-reduced surface, as shown in Figure 1b.

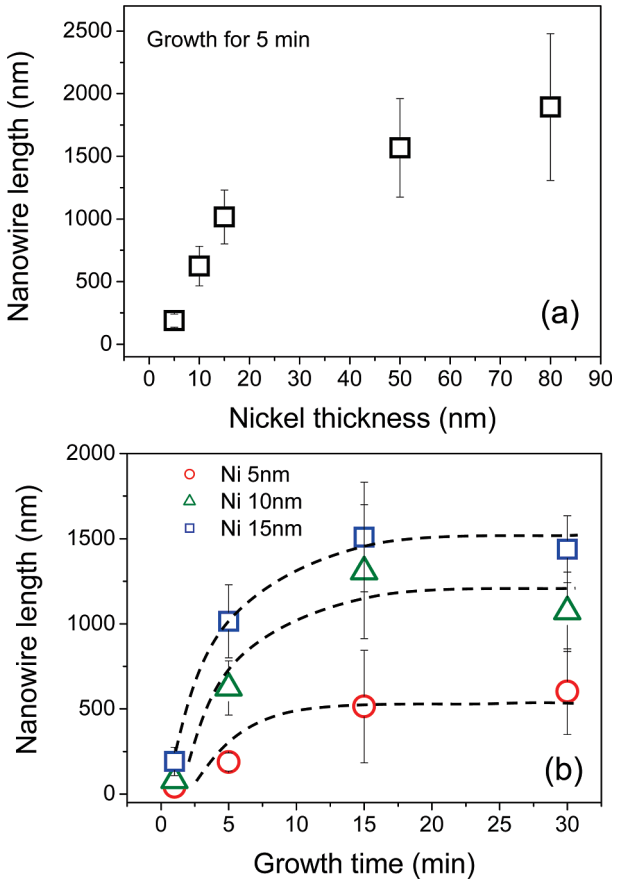

Figure 4. (a) Variation of the $NiSi_x$ nanowire lengths for the 5 min growth when varying the thickness of the Ni underlayers from 5 to 80 nm. (b) Variation of the $NiSi_x$ nanowire lengths on the 5, 10, and 15 nm thick Ni when varying the growth time up to 30 min. Dotted lines are guides for clarity.

In summary, we report a controllably reproducible and spontaneous growth of single-crystalline $NiSi_x$ nanowires by SiH_4 CVD on NiO_x/Ni seed layers without employing catalytic nanocrystals. We show experimental evidence that the presence of the NiO_x overlayer on Ni seed layers is critical to promote the one-dimensional growth of $NiSi_x$ single crystals in a self-organized manner during the SiH_4−Ni reactions. Specifically, we discussed the roles of the NiO_x overlayers on the top of the Ni seed layers for the spontane-

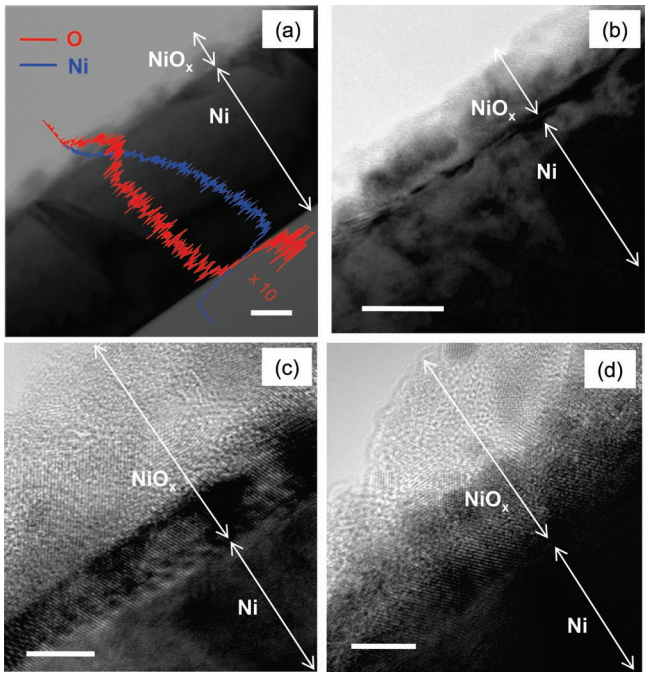

Figure 5. Cross-sectional TEM images of 10 min oxidized Ni layers. (a) Energy dispersive X-ray data across the NiO_x/Ni interface is overlaid on the scanning TEM image. The scale bar is 50 nm. (b−d) TEM images at different magnifications of different spots from panel a. The scale bar of panel b is 20 nm, and the scale bar of panels c and d is 5 nm.

ous growth of $NiSi_x$ nanowires as the diffusion barrier for the kinetically and spatially limited Ni supply for the reaction. Then the spontaneous nanowire formation can be understood with the limited nucleation during the vapor−solid reactions in the low supersaturation limit of the solid-phase of Ni controlled by NiO_x. We argue that our synthetic method, employing the bilayers of transition metal and their oxides as the seed layers, provide implication for the spontaneous growth of metal−silicide nanowires in general.

Acknowledgment. This research was supported by Nano R & D program through the Korea Science and Engineering Foundation funded by the Ministry of Science & Technology (2006-04921 and 2007-02864), the "System IC 2010" project of the Korea Ministry of Commerce, Industry, the MOST-AFOSR NBIT 2007 Program, the Korean Research Foundation Grant from the Korean Research Foundation Grant from the Korean Government (KRF-2005-005-J13103) and the POSTECH Core Research Program.

Supporting Information Available: This material is available free of charge via the Internet at http://pubs.acs.org.

References

(1) Wagner, R. S.; Eliis, W. C. *Appl. Phys. Lett.* **1964**, *4*, 89.
(2) Morales, A. M.; Lieber, C. L. *Science* **1998**, *279*, 208.
(3) Recent examples are found in the following: (a) Persson, A. I.; Larsson, M. W.; Stenström, S.; Ohlsson, B. J.; Samuelson, L.; Wallenberg, L. R. *Nat. Mater.* **2004**, *3*, 677. (b) Wang, Y.; Schmidt, V.; Senz, S.; Gosele, U. *Nat. Nanotechnol.* **2006**, *1*, 186. (c) Kodambaka, S.; Tersoff, J.; Reuter, M. C.; Ross, F. M. *Science* **2007**, *316*, 729.
(4) Numerous examples can be found in the following review article: Xia, Y.; Yang, P.; Sun, Y.; Wu, Y.; Mayers, B.; Gates, B.; Yin, Y.; Kim, F.; Yan, H. *Adv. Mater.* **2003**, *15*, 353.
(5) Examples of oxide-assisted nanowire growth can be found in the following: (a) Wang, N.; Tang, Y. H.; Zhang. Y. F.; Lee, C. S.; Lee, S. T. *Phys. Rev. B* **1998**, *58*, R16024. (b) Zhang, Y.; Wang, N.; Gao, S.; He, R.; Miao, S.; Liu, L.; Zhu, J.; Zhang, X. *Chem. Mater.* **2002**, *14*, 3564.
(6) Wu, Y.; Xiang, J.; Yang, C.; Lu, W.; Lieber, C. M. *Nature* **2004**, *430*, 61.
(7) Decker, C. A.; Solanki, R.; Freeouf, J. L.; Carruthers, J. R.; Evans, D. R. *Appl. Phys. Lett.* **2004**, *84*, 1389.
(8) Kim, J.; Anderson, W. A. *Nano Lett.* **2006**, *6*, 1356.
(9) Kim, C.-J.; Kang, K.; Woo, Y. S.; Ryu, K.-G.; Moon, H.; Kim, J.-M.; Zang, D.-S.; Jo, M.-H. *Adv. Mater.* **2007**, *19*, 3637.
(10) Chueh, Y.-L.; Ko, M.-T.; Chou, L.-J.; Chen, L.-J.; Wu, C.-S.; Chen, C.-D. *Nano Lett.* **2006**, *6*, 1637.
(11) Ouyang, L.; Thrall, E. S.; Deshmukh, M. M.; Park, H. *Adv. Mater.* **2006**, *18*, 1437.
(12) Schmitt, A. L.; Bierman, M. J.; Schmeisser, D.; Himpsel, F. J.; Jin, S. *Nano Lett.* **2006**, *6*, 1617.
(13) Song, Y.; Schmitt, A. L.; Jin, S. *Nano Lett.* **2007**, *7*, 965.
(14) Seo, K.; Varadwaj, K. S. K.; Mohanty, P.; Lee, S.; Jo, Y.; Jung, M.-H.; Kim, J.; Kim, B. *Nano Lett.* **2007**, *7*, 1240.
(15) Dubois, L. H.; Nuzzo, R. G. *J. Vac. Sci. Tech., A* **1984**, *2*, 441.
(16) Rodriguez, J. A.; Hanson, J. C.; Frenkel, A. I.; Kim, J. Y.; Pérez. M. *J. Am. Chem. Soc.* **2002**, *124*, 346.
(17) Schmitt, A. L.; Zhu, L.; Schmeiser, D.; Himpsel, F. J.; Jin, S. *J. Phys. Chem. B* **2006**, *110*, 18142.
(18) Schmitt, A. L.; Jin, S. *Chem. Mater.* **2007**, *19*, 126.
(19) Zhang, R. Q.; Lifshitz, Y.; Lee, S. T. *Adv. Mater.* **2003**, *15*, 635.
(20) Gambino, J. P.; Colgan, E. G. *Mater. Chem. Phys.* **1998**, *52*, 99.
(21) d'Heurle, F. M.; Gas, P. *J. Mater. Res.* **1986**, *1*, 205.
(22) Kursumovic, A.; Tomov, R.; Huhne, R.; Glowacki, B. A.; Everts, J. E.; Tuissi, A.; Villa, E.; Holzapfel, B. *Physica C* **2003**, *385*, 337.

NL072326C